INTERNATIONAL JOURNAL OF OPTIMIZATION IN CIVIL ENGINEERING
Int. J. Optim. Civil Eng., 2022; 12(2):245-278

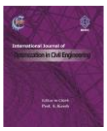

QUANTUM VERSION OF TEACHING-LEARNING-BASED OPTIMIZATION ALGORITHM FOR OPTIMAL DESIGN OF CYCLIC SYMMETRIC STRUCTURES SUBJECT TO FREQUENCY CONSTRAINTS

A. Kaveh[*, †,1], M. Kamalinejad[2], K. Biabani Hamedani[1] and H. Arzani[2]

[1] *School of Civil Engineering, Iran University of Science and Technology, Tehran, Iran*
[2] *Department of Civil Engineering, Shahid Rajaee Teacher Training University, Tehran, Iran*

ABSTRACT

As a novel strategy, Quantum-behaved particles use uncertainty law and a distinct formulation obtained from solving the time-independent Schrodinger differential equation in the delta-potential-well function to update the solution candidates' positions. In this case, the local attractors as potential solutions between the best solution and the others are introduced to explore the solution space. Also, the difference between the average and another solution is established as a new step size. In the present paper, the quantum teacher phase is introduced to improve the performance of the current version of the teacher phase of the Teaching-Learning-Based Optimization algorithm (TLBO) by using the formulation obtained from solving the time-independent Schrodinger equation predicting the probable positions of optimal solutions. The results show that QTLBO, an acronym for the Quantum Teaching- Learning- Based Optimization, improves the stability and robustness of the TLBO by defining the quantum teacher phase. The two circulant space trusses with multiple frequency constraints are chosen to verify the quality and performance of QTLBO. Comparing the results obtained from the proposed algorithm with those of the standard version of the TLBO algorithm and other literature methods shows that QTLBO increases the chance of finding a better solution besides improving the statistical criteria compared to the current TLBO.

Keywords: quantum-inspired evolutionary algorithm; teaching-learning-based optimization; population-based algorithm; circulant truss; quantum behaved particles; quantum teacher; frequency constraint.

Received: 10 January 2022; Accepted: 11 April 2022

[*] Corresponding author: School of Civil Engineering, Iran University of Science and Technology, Narmak, Tehran, P.O. Box 16846-13114, Iran
[†]E-mail address: alikaveh@iust.ac.ir (A. Kaveh)

1. INTRODUCTION

The development of optimization methods based on meta-heuristic approaches provides efficient tools for solving real complex problems in many disciplines such as engineering, computer science, and mathematics. During the recent two decades, Genetic Algorithm (GA) [1], Ant Colony Optimization (ACO) [2], Particle Swarm Optimization (PSO) [3], etc. have been frequently employed by scientists from different fields to solve various problems. Simulated annealing (SA) [4], Shuffled Complex Evolution (SCE) [5], Artificial Bee Colony (ABC) [6], Shuffled Frog-Leaping Algorithm (SFLA) [7], Cuckoo Search (CS) [8], etc. have been frequently used in vast researchers' articles. Moreover, developing recent optimization methods, such as Differential Evolution (DE) [9], Teaching-Learning-based Optimization (TLBO) [10], Bat Algorithm (BA) [11], and Grey Wolf Optimizer (GWO) [12], etc. have depicted the attempts in this area.

Simplicity, flexibility, stochastic mechanism, and local optimum point avoidance surge the usage of meta-heuristics methods. Based on the No Free Lunch (NFL) theorem [13], no meta-heuristic is suited for solving all different optimization problems. Therefore, although a particular meta-heuristic algorithm solves various problems with excellent performance, it shows poor results on different complexed problems. Therefore, finding new methods interestingly remains active and leads to better novel algorithms or even improved ones with some advanced strategy.

Kaveh et al. have introduced several optimization algorithms and enhanced methods applied to the various structural design and analysis problems such as Charged System Search (CSS) [14], Ray Optimization (RO) [15], Dolphin Echolocation (DE) [16], Colliding Bodies Optimization (CBO) [17], Water Evaporation Optimization (WEO) [18], Thermal Exchange Optimization (TEO) [19], Water Strider Algorithm (WSA) [20], Quantum evolutionary algorithm hybridized with Enhanced colliding bodies for optimization (QECBO) [21].

In general, research presented in the field of meta-heuristic algorithms can be divided into three categories: proposing a new optimization algorithm, improving the current version of optimization methods, and finally applying them to different problems. In terms of Optimization algorithm improvement, meta-heuristic algorithms must establish the right balance between these two phases, local and global search, to escape a local optimum. Some changes are utilized to improve the optimization algorithms' performance, such as hybridization techniques or new step size formulation. Various algorithms are employed and combined to produce a new enhanced version of the current algorithm consisting of features of two or more methods [21-31].

Due to altering some situations compared to primary conditions, computations and analysis are inevitable to ensure quality. The universe is an extended computer from the viewpoint of Philip Ball and some other physicists. Seth Lloyd has estimated the number of computations our universe has done since the big bang [32]. Although the input states and output states are orthogonal in a traditional computer, states can be superposition states in a quantum computer. Each quantum transformation is a unitary one and vice versa. The quantum computers can remarkably give a solution for a particular problem after some measurement at the end of the computation. Related societies utilize Grover's quantum search and Shor's number factoring algorithm as milestones to spur a flurry of activity. The

topic, quantum search, verified by various experiments, has a leading role in quantum computation due to the crucial role of search in many fields, especially computer science [33].

The high potential of Quantum-inspired evolutionary algorithms driven by the interaction between quantum computing and evolutionary algorithms has created new methods to find novel optimization algorithms. The original version of the quantum evolutionary algorithm (QEA) uses Q-bit individuals in binary code similar to genes in the conventional genetic algorithm and quantum computing's concept and principles. Nevertheless, QEA is not a quantum algorithm but a novel evolutionary algorithm [34].

The approach of quantum-behaved particles, as a novel strategy, uses uncertainty law and a distinct formulation obtained from solving the time-independent Schrodinger differential equation in the delta-potential-well function to update the solution candidates' positions. The new formulation defines the local attractors as possible solutions between the best solution and the others to explore the whole solution space domain. Also, the mentioned formulation employs the difference between the average solution and others as a new step size. Both local attractors and new step sizes guarantee diversification besides intensification. Using the probability rules related to the quantum probability density function creates a new formulation for updating the position of solutions, considering the mean of solutions and the best one through an iterative process. As a helpful framework, using quantum-behaved particles could improve the quality of solutions during a particular optimization algorithm with efficient local and global search. The collision bodies optimization (CBO), which was presented in 2014 by Kaveh and Mahdavi [17], has been recently improved by using quantum-behaved particle features in QECBO [21] to cope with suffering local optimum points in some NP-hard problems. Obtained results show that QECBO enhances ECBO's performance with efficient searching. It seems that the QECBO utilizes the rules of uncertainty inside classical mechanics.

In the present paper, the quantum teacher phase is introduced to the Teaching-Learning-Based Optimization algorithm (TLBO) to enhance the performance of TLBO in such complex problems. The TLBO algorithm is one of the most efficient population-based meta-heuristic developed by Rao et al. in 2011 [10], which simulates the classroom's traditional teaching-learning phenomenon. Although the obtained results from the literature unveiled that the TLBO could be an excellent optimization method for some problems, it suffers from getting stuck in local solutions in other cases, as mentioned in the No Free Lunch (NFL) theorem [13] for another method. As an essential process, teaching-learning impacts improving each member's knowledge in the various community. TLBO's learning process could be found in several societies of humans and animals. The algorithm is made of the teacher and learner phases as two fundamental learning modes. TLBO is a population-based algorithm where a group of students (i.e., learners) is considered a population, and different subjects offered to the learners are analogous to the different design variables of the optimization problem. The learner's results are analogous to the fitness value of the optimization problem. Population-based optimization methods use probabilistic and stochastic environments as a prominent evolutionary and swarm intelligence-based algorithm class. These methods work with tuning some inherent parameters such as population size, the number of generations, and others. The TLBO algorithm also works with the tuning of the population size and the number of generations only. Rao and Patel

explained that TLBO is an optimization method with less-parameter tuning [35], although Črepinšek et al. [36] had expressed another idea.

QTLBO, an acronym for the Quantum Teaching-Learning-Based Optimization, is introduced by defining the quantum teacher Phase instead of the former definition, which updates the solution positions using quantum-behaved particles. The QTLBO has been recently proposed by Kaveh et al. [37] to consider the quantum framework to improve a specific method. Compared to QECBO [21], which uses the updated results of ECBO as local attractors in quantum formulation just after ECBO up-gradation, QTLBO utilizes a new formulation based on quantum behaved particles to update the position of learners in the teacher phase of the TLBO. QTLBO attempts to move the solutions toward the promised solution space or the best one.

Two circulant spatial domes with multiple frequency limitations are considered To evaluate the performance of the quantum variant of TLBO. The reason for choosing these optimization problems is their highly nonlinear, non-convex, and discontinuous search spaces with several local optima [38]. The most common problem with frequency-constrained optimization seems to be the high sensitivity of vibration modes to shape modifications, which means that vibration modes can switch during the optimization process, which causes convergence difficulties [39]. In the past few decades, frequency-constrained optimization problems have attracted the attention of many researchers. Bellagamba and Yang [40] were one of the first researchers to study the minimum-mass design of truss structures with natural frequency constraints. Grandhi and Venkayyat [41] presented a design optimization algorithm for structural weight minimization with multiple frequency constraints. Tong and Liu [42] presented an optimization procedure for the minimum weight optimization of truss structures subjected to constraints on stresses, natural frequencies, and frequency responses. Sedaghati et al. [43] compared the performance of the displacement and force methods to optimize truss and beam structures with frequency constraints. Lingyun et al. [44] used an enhanced genetic algorithm to optimize the truss shape problems. Gomes [45] investigated the performance of a particle swarm optimization (PSO) algorithm in truss optimization with frequency constraints. In a similar work, Miguel and Fadel Miguel [46] used the harmony search (HS) and the firefly algorithm (FA) to solve truss shape and size optimization with frequency constraints. Kaveh et al. [47] proposed enhanced forensic-based investigation (EFBI) algorithm for weight minimization of truss structures with frequency constraints. Kaveh et al. [48] proposed improved slime mould algorithm (ISMA) to solve dome-shaped truss optimization problems with frequency constraints. Kaveh and Ilchi Ghazaan [49] used the vibrating particles system (VPS) algorithm for truss optimization with multiple natural frequency constraints. Kaveh and Zolghadr [50] presented a study where the cyclical parthenogenesis algorithm (CPA) was employed for layout optimization of truss structures with frequency constraints. Kaveh and Zolghadr [51] reviewed different metaheuristic optimization techniques utilized for structural optimization problems with frequency constraints. Recently, Kaveh et al. [52] studied the performance of some metaheuristics in frequency-constrained truss. In this paper, a quantum version of the TLBO algorithm is developed. The effectiveness of the proposed algorithm is investigated through two truss optimization problems with multiple frequency constraints. The results are compared with those of the standard TLBO and some other methods reported in the literature.

The rest of this paper is organized as follows: In section 2, first, a brief explanation of the TLBO and an overview of the Quantum mechanics principles with QTLBO formulation are presented. Next, the QTLBO algorithm steps and its flowchart are presented. In Section 3, various design examples are assessed. Finally, Section 4 concludes the results of the paper and future works.

2. MATERIALS AND METHODS

2.1 Teaching-learning-based optimization (TLBO) algorithm

TLBO, which is derived from the traditional education process in classrooms, includes two main parts. The first part is related to selecting the best solution (teacher) and sharing knowledge between the teacher and other solutions in the teacher phase. The second one determines the learner's process to find better solutions by using knowledge between a particular candidate and the accidentally selected one. These two parts play leading roles in the TLBO algorithm. Intensification and diversification are guaranteed in the teacher and learner phases, respectively.

The optimization process of TLBO starts with a set of random populations called students. After the primary evaluation of solutions, the best solution is assumed to be the teacher. The knowledge is shared between the teacher and other solutions in the teacher phase. The newly updated solutions are evaluated, and the better solutions are chosen and replaced with the old ones. After that, each solution's awareness is updated via sharing featuring another randomly selected solution. Like the teacher step, a replacement strategy is applied to keep the old learners or replace them with newly generated ones after the learner phase. The TLBO algorithm steps are presented and formulated as follows [10]:

Step one (forming the initial population): In the TLBO algorithm, the initial candidate solutions can be considered a class with *nS* students. The set of randomized students (*S*) can be produced through the following equation:

$$S = Lb + (Ub - Lb) \times rand(nS, nVar) \tag{1}$$

where nS is the number of students, nVar is the number of design variables, and Lb and Ub are the lower and upper bound vectors of the design variables.

Step two (teacher phase): First, the students are evaluated, and their corresponding penalized objective function vector ($PFit$) is generated. Next, the best student (the student with the best-penalized objective function value) is chosen as the teacher (T). A step size updates the students toward their teacher. The step size is obtained based on the teacher's knowledge and the average knowledge of all the students (AveS). The teacher phase is formulated as follows:

$$\begin{gathered} stepsize_i = T - TF_i \times Ave_S \\ newS = S + rand_{i,j} \times stepsize \\ i = 1,2,\dots,nS \text{ and } j = 1,2,\dots,nVar \end{gathered} \tag{2}$$

The term of $stepsize_i$ is the step size of ith student, $newS$ is the vector of new students, $rand_{i,j}$is a random number chosen from the interval of [0, 1] and the teacher factor (TF_i) is considered to change the effect of the teacher's knowledge on the class's average, which can be either 1 or 2. The value of TF_i is not given as an input to the algorithm, and the algorithm randomly decides its value. The schematic generation of new solutions in the teacher phase of TLBO presented in Fig. 1 reveals that the probable region of new solutions is likely between two vectors of the current solution (S) and randomized step size. Adopting a strategy like hybridization or other improvements mentioned in QTLBO might be beneficial for exploring a broad probable region of solution space.

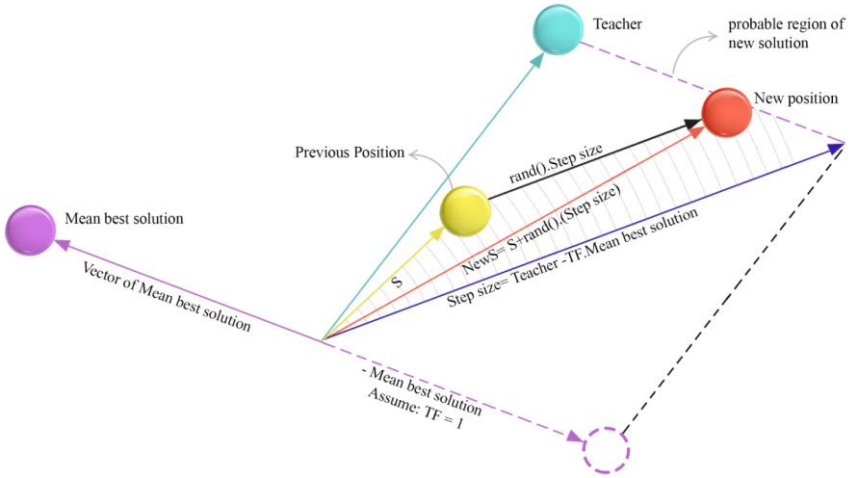

Figure 1. A schematic of generating a new position in the TLBO at the teacher phase

Step three (replacement strategy): In this step, newly generated students are evaluated and replaced with their corresponding old ones in a simple greedy manner. In this way, the newly generated student with a better-penalized objective function is preferred to his corresponding old one. Therefore, a new class with nS students is formed.

Step four (learner phase): In the learner phase, firstly, each student randomly chooses another one (*Srs*) except himself. Next, the student shares his knowledge with the randomly selected one. The student moves toward the other selected student if the other selected one has more knowledge than him ($PFit_i < PFit_{rs}$). The learner phase can be formulated as follows:

$$\begin{gathered} stepsize_i = \begin{cases} S_i - S_{rs};\ PFit_i < PFit_{rs} \\ S_{rs} - S_i;\ PFit_i \geq PFit_{rs} \end{cases} \\ newS = S + rand_{i,j} \times stepsize \\ i = 1,2,\dots,nS \text{ and } j = 1,2,\dots,nVar \end{gathered} \tag{3}$$

Initialization:
Set the algorithm parameters: *nS*, *MaxNFEs*.
Generate random initial candidate solutions or elements (*S*).
Evaluate the set of elements (candidate solutions).
$i = 0$; $NFEs = 0$;
Cyclic body of the algorithm:
While *NFEs < MaxNFEs/k or termination criteria is satisfied*
Step 1: Generate the new solutions (*newS*) based on the teacher phase.
Step 2: Evaluate the newly generated solutions (*newS*) and apply replacement strategy between old and new candidates.
Update the number of function evaluations ($NFEs = NFEs + nS$).
Step 3: Generate the new solutions (*newS*) based on the learner phase.
Step 4: Evaluate the newly generated subsets (*newS*) and apply replacement strategy between old and new ones.
Update the number of function evaluations ($NFEs = NFEs + nS$).
Step 5: Monitor the best element found by the TLBO algorithm so far.
EndWhile

Figure 2. The pseudo-code of the TLBO

Step five (replacement strategy): The replacement strategy is performed again.

Step six (termination criteria): If the algorithm's termination criterion is satisfied, the algorithm is terminated. Otherwise, go to step two. The pseudo-code of the TLBO algorithm is provided in Fig. 2.

2.2 Quantum formulation

Compared to classical mechanics, Quantum mechanics provide a theoretical and probable definition of particle location in space. Hence, the wave function $\Psi(x,t)$, of the particle, is obtained by solving the Schrödinger equation [53]:

$$i\hbar\frac{\partial\Psi}{\partial t} = -\frac{\hbar^2}{2m}\frac{\partial^2\Psi}{\partial^2 t} + V\Psi \tag{4}$$

which i is the square root of -1, V is the potential energy function, and ħ is the Plank's constant- or rather, and his original constant (h) divided by 2π:

$$\hbar = \frac{h}{2\pi} = 1.054573 \times 10^{-34}\ js \tag{5}$$

The Schrödinger equation has the same role in Newton's second law

As Born's statistical interpretation of wave function says that $|\Psi(x,t)|^2$ gives the probability of finding the particle at point x, at time t:

$$|\Psi(x,t)|^2\ dx = \left\{\begin{matrix}\text{probability of finding the particle} \\ \text{between } x \text{ and } x+dx \text{ at time t}\end{matrix}\right\} \tag{6}$$

Figure 3 shows a typical wave function. It would be pretty likely to find the particle in point *A*'s vicinity and relatively unlikely to find it near point *B* because the particle's got to be somewhere.

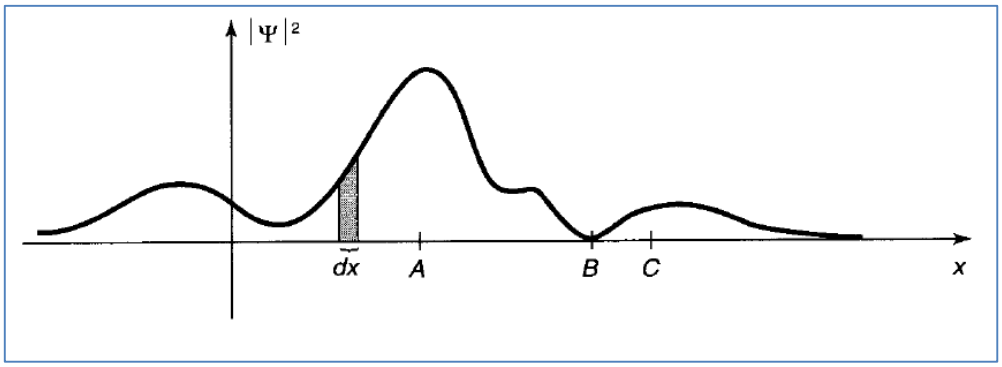

Figure 3. A typical wave function

The Schrodinger equation can be solved by the method of separation of variables.

$$\Psi(x,t) = \psi(x).\varphi(t) \tag{7}$$

where ψ is a function of *x* alone, and φ is a function of *t* alone. The process of separation creates the Eq. (8):

$$i\hbar \frac{1}{\varphi}\frac{d\varphi}{dt} = -\frac{\hbar^2}{2m}\frac{1}{\psi}\frac{d^2\psi}{dx^2} + V = E \tag{8}$$

The second part of Eq. (8) is called the time-independent Schrodinger equation. It is necessary to specify the potential function *V(x)* to solve Eq. (8). One of the most well-known potential functions is the one-dimensional Delta potential function, which uses the Dirac delta function definition. After solving the time-independent Schrodinger equation, we can calculate each particle's existence probability in quantum space. The Dirac delta function, $\delta(x)$, is defined as follows:

$$\delta(x) = \begin{cases} 0 \text{ if } x \neq 0 \\ \infty \text{ if } x = 0 \end{cases} \text{ with } \int_{-\infty}^{+\infty} \delta(x)dx = 1 \tag{9}$$

This function is an infinitely narrow spike at the origin, whose area is equal to unity (see Fig. 4).

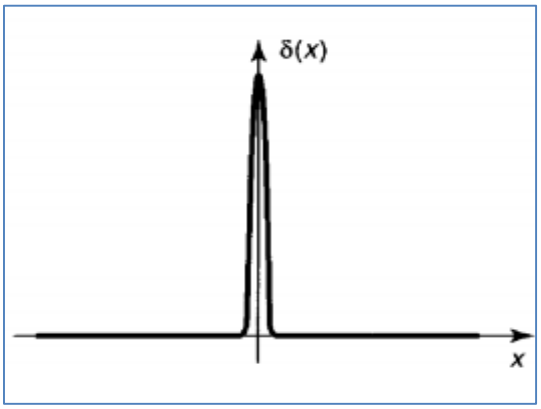

Figure 4. The Dirac delta function

Notice that $\delta(x-a)$ would be a spike of a unit area at the point a. If we multiply $\delta(x-a)$ by an ordinary function *f*(*x*), it is the same as multiplying by *f* (*a*) [53]:

$$f(x)\,\delta(x-a) = f(a)\,\delta(x-a) \tag{10}$$

Since the product is zero except at point *a*. In particular,

$$\int_{-\infty}^{+\infty} f(x)\,\delta(x-a)dx = \int_{-\infty}^{+\infty} f(a)\,\delta(x-a)dx = f(a) \tag{11}$$

Let us consider the potential of the form:

$$V(x) = -\alpha\,\delta(x) \tag{12}$$

where α is constant. After replacing Eq. (8) with Eq. (12), The Schrodinger equation reads:

$$-\frac{\hbar^2}{2\mathrm{m}}\frac{d^2\psi}{dx^2} - \alpha\,\delta(x)\psi = E\psi \tag{13}$$

or

$$\frac{d^2\psi}{dx^2} + k^2\psi = 0 \tag{14}$$

where

$$k = \sqrt{-2mE/\hbar^2} \tag{15}$$

This potential yields both bound states ($E < 0$) and scattering states ($E > 0$); we will look first at the bound states. In the region $x < 0$, $V(x) = 0$, and E is negative, by assumption, so k is real and positive. The general solution to Eq. (14) is

$$\psi = Ae^{-kx} + Be^{kx} \tag{16}$$

In Eq. (16), the first term blows up as x→ −∞, so we must choose $A = 0$

$$\psi = Be^{kx}, \qquad x < 0 \tag{17}$$

In the region $x > 0$, $V(x)$ is again zero, and the general solution is of the form:

$$\psi = Ce^{-kx} + De^{kx} \tag{18}$$

This time it is the second term that blows up (as x→ +∞), so

$$\psi = Ce^{-kx}, \qquad x > 0 \tag{19}$$

It remains only to stitch these two functions together, using the appropriate boundary conditions at $x = 0$:

1. ψ is always continuous, and
2. $d\psi/dx$ is continuous except at points where the potential is infinite.

In this case, the first boundary condition indicates that C = B, so

$$\psi(x) = \begin{cases} Be^{kx}, & x < 0 \\ Be^{-kx}, & x > 0 \end{cases} \tag{20}$$

First, we consider a particle in one-dimensional space. With point p (local attractor) at the center of the potential well, the potential energy of the particle in a one-dimensional Delta potential well is represented as:

$$V(x) = -\alpha\, \delta(x - p) = -\alpha\, \delta(y) \tag{21}$$

Letting $x - p = y$, with m being the mass of the particle. The idea is to integrate the Schrodinger equation, from $-\varepsilon$ to $+\varepsilon$, and then take the limit as $\varepsilon \to 0$:

$$\begin{gathered} \int_{-\varepsilon}^{+\varepsilon} \left(-\frac{\hbar^2}{2\mathrm{m}} \frac{d^2\psi(y)}{dy^2} - \alpha\, \delta(y)\psi(y)\right) dy = \int_{-\epsilon}^{+\varepsilon} (E\psi(y)) dy = 0 \\ \psi'(0^+) - \psi'(0^-) = -\alpha \frac{2m}{\hbar^2} \psi(0) \\ -2Bk = -\alpha \frac{2m}{\hbar^2} B \end{gathered} \tag{22}$$

Thus:

$$\begin{gathered} k = \frac{\alpha m}{\hbar^2} \\ E = E_0 = -\frac{\hbar^2 k^2}{2\mathrm{m}} = -\frac{\alpha^2 m}{2\hbar^2} \end{gathered} \tag{23}$$

Determining the constants so that the function $\psi(y)$ satisfy normalization condition

$$\int_{-\infty}^{+\infty} |\psi(y)|^2 dx = \frac{B^2}{k} = 1$$
$$\mathrm{B} = \sqrt{k}\,, \qquad L = \frac{1}{k} = \frac{\hbar^2}{\alpha m} \tag{24}$$

L is related to the characteristic length of the delta potential well, which determines each particle's search scope. It means the domain of changes of each particle can be recognized by an interval on both sides of the mean best point (p_{mean}). This point is the mean of all particles' dimensions. We can then represent the normalized wave function as

$$\psi(y) = \frac{1}{\sqrt{L}} e^{-\frac{|y|}{L}} \tag{25}$$

Evaluating fitness needs precise information about the position of the body. However, the quantum state function $\psi(y)$ or $|\psi(y)|^2$ gives the probability density function that the particle appears at position y relative to p. Thus one needs to calculate the classical state from the collapsing quantum state. The procedure of simulation is described as follows. Assume s, which is the random number on $(0,1/L)$, is the probability of the existence of a quantum body in a particular position p [53].

$$s = random\left(0, \frac{1}{L}\right) = \frac{1}{L} random(0,1) = \frac{1}{L}.u$$
$$s = |\psi(y)|^2 = \frac{1}{L}\,.e^{-2\frac{|y|}{L}} \tag{26}$$
$$u = e^{-2\frac{|y|}{L}} \;\rightarrow\; |y| = \pm\frac{L}{2}\ln(\frac{1}{u}) \rightarrow\; x - p = \pm\frac{L}{2}\ln(\frac{1}{u})$$

In the above equation, p, which is probably the particle's location in quantum space, is a local attractor. The local attractor is used to define a new randomized location between the best solution and the current one for better diversification in each iteration. Also, u is a random number in the interval of (0, 1), which determines the existence probability of the selected local attractor point (p) as a solution. The length of the potential well (L) is equal to a fraction of the distance between the mean best (p_{mean}) and current position of the particle ($x_i{}^{old}$) which provides efficient moving toward a probable optimal solution. Then:

$$p_{mean} = \frac{1}{n}.(x_1{}^{old} + x_2{}^{old} + \cdots + x_{2n}{}^{old}) \tag{27}$$
$$L = 2\beta.|p_{mean} - x^{old}| \tag{28}$$

From the substitution of Eqs. (26) by (28), we can obtain the following general equation to update the position of the particles:

$$x_i^{new} = p \pm \beta . |p_{mean} - x_i^{old}| . \ln(\frac{1}{u}) \tag{29}$$

which i=1, 2, 3,… is the number of particles, x^{old} and x^{new} are the position of particles before and after updating, respectively. The new equation (Eq. (29)) plays a leading role in the quantum vision of a population-based algorithm. In Eq. (29), the u are random numbers between [0, 1]. Also, the coefficient of β In Eq. (29) controls the convergence of the algorithm. It starts from 1 to 0.5 from the first iteration to the maximum iteration.

The behavior of a single particle in a quantum framework depends on how the β value is selected. Therefore, random simulation is performed to assess the sensitivity analysis. The value of β for simulations is assumed to be in the range [0.5, 2.1], and the maximum number of iterations is equal to the number of steps required to converge to preassumed p. In this simulation, the value of $p = 0$ and the particle's position in the first step are assumed to be $x_0 = 1000$. When the random simulation is performed on Matlab, the logarithmic value of the current position x_n on the vertical axis is displayed versus the number of iterations on the horizontal axis. As shown in Figures 5 to 7, the new positions of the solutions x_n converge to assumed values of p if β ≤1.775; otherwise, do not converge to p.

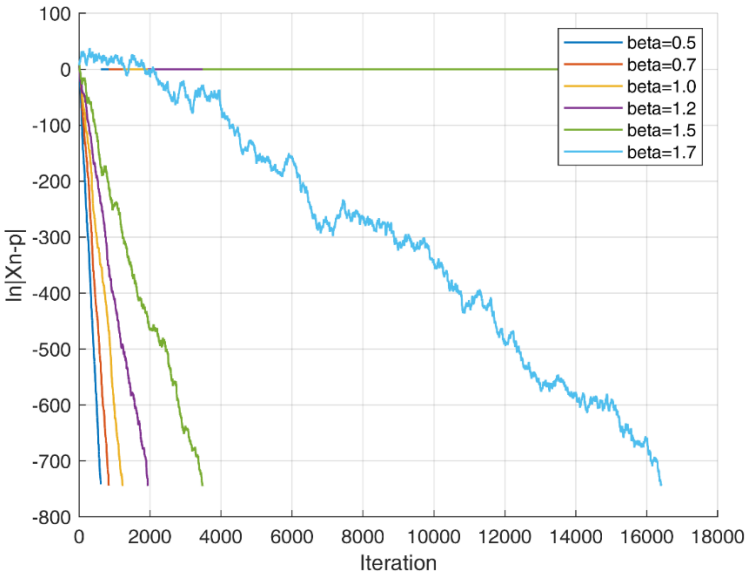

Figure 5. Changes of $\ln|(p - x_n)|$ relative to the number of iterations for different values of β

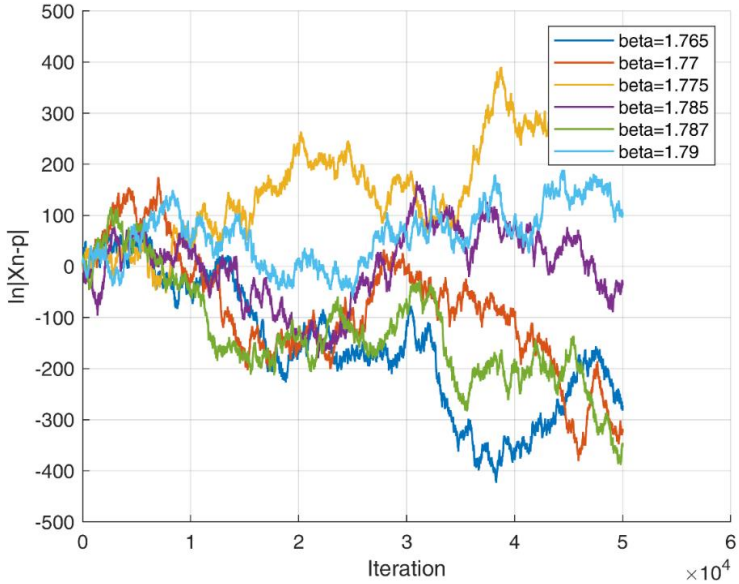

Figure 6. Changes of $\ln|(p - x_n)|$ relative to the number of iterations for different values of β

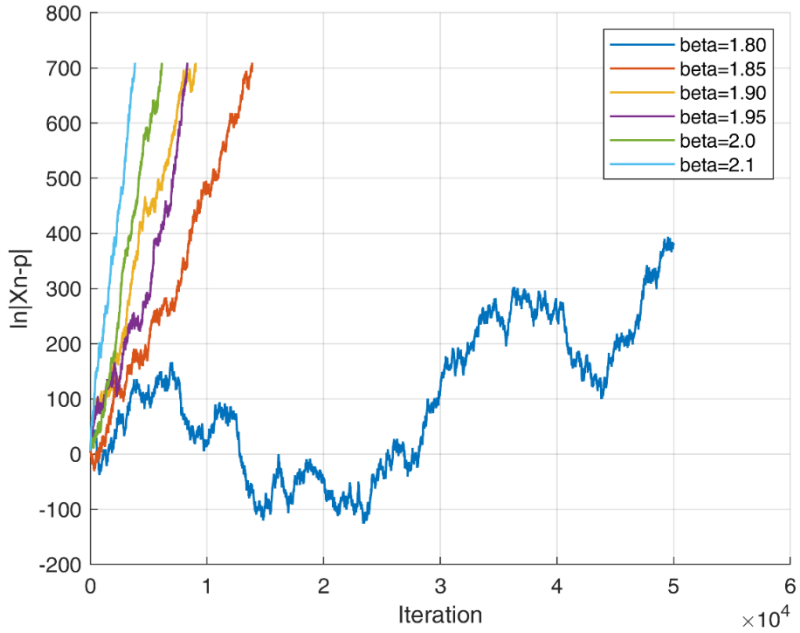

Figure 7. Changes of $\ln|(p - x_n)|$ relative to the number of iterations for different values of β

It should be noted that the β parameter strongly converges the algorithm process in small quantities. Therefore, to ensure convergence, β should have values close to 0.5 at the end of the algorithm iterations. In contrast, β in the initial steps provides higher values to achieve the appropriate divergence for effective search in the algorithm. Conclusively, the parameter

of β is assumed to decrease gradually from 1.0 to 0.5, which guarantees convergence in the final iterations besides divergence in the initial steps of the algorithm.

$$\beta = 1 - (1 - 0.5) * (\frac{iter}{MaxIteratin}) \tag{30}$$

2.3 Quantum formulation

As an improved optimization algorithm, QTLBO, recently proposed by Kaveh et al., uses quantum-behaved particles' features to enhance the performance of TLBO in solving the NP-hard problems, which have many local optimum spots in search space [37]. The teacher phase of TLBO is modified using the quantum formulation obtained from solving the time-independent Schrodinger differential equation in the delta-potential function to update the solution candidates' positions. Indeed, in the current version of TLBO, after defining the teacher in each iteration, all the current solutions with the randomized step size move toward the best solution using teacher factor parameter 1 or 2. In the early stages of the optimization process, TLBO reveals the best diversification because of differences between the best solution and the best mean solution. However, in the late iterations, decreasing the difference between the teacher and mean solution at the teacher phase besides decreasing the solution differences because of convergence cause less dynamic solutions in both phases of TLBO. Any solutions updates in TLBO use the randomized step size defined with the difference between the teacher solution and the mean best one. Hence, it is necessary to mention that the old solutions in each iteration of the teacher phase remain fixed without any local alteration till the new solution formulation creates the new ones. This study proposes changing the teacher phase of TLBO and defining a local attractor between the best solution and the other using the quantum-behaved particle formulation. The quantum teacher phase concept in QTLBO increases the chance of finding a better solution due to better diversification and intensification than TLBO because of quantum searching and the inclination toward the best solution. Any solutions updates in TLBO use the randomized step size defined with the difference between the teacher solution and the mean best one.

Quantum vision of teacher, which utilizes local attractors (p), produce an efficient local search around the point of the best solution. Also, considering local attractors, how to define their formulation improves the diversification of the algorithm while converging to the best solution. For instance, QECBO defines the local attractors (p) same to updated solutions of ECBO [21], while QTLBO utilizes Eq. (31) to define a probable solution between the best solution and the current candidate, which likely has more chance to be a more probable better solution than the current one. In Eq. (31) the c_1 and c_2 are random numbers between [0, 1].

$$p_{i,local\ atractor} = \frac{(c_1.\ x_{i,current} + c_2.\ x_{Global\ Best})}{c_1 + c_2} \tag{31}$$

In terms of providing a better chance to experience large or small increment, $\ln(\frac{1}{u})$ fluctuates approximately in the range of (0, 10). Figure 8 shows the changes of $\ln(\frac{1}{u})$ on the vertical axis versus 1000 random number of u in the range of [0, 1] on the horizontal line.

The recent term of $\ln(\frac{1}{u})$ in Eq. (29) undergoes different values, which could surge the diversification rate of QTLBO. Figure 9 shows the dynamic of $\beta.\ln(\frac{1}{u})$ for a two-dimension problem in 100 consecutive iterations. In Eq. (29), the term of $\beta.\ln(\frac{1}{u})$ creates the various increments that make current solutions escape from local optimums. This new approach helps the solutions to experience all promised regions between the best and worst solutions. As the results of this paper will reveal, QTLBO seems capable of exploring all space of solution more efficiently than the standard version of TLBO.

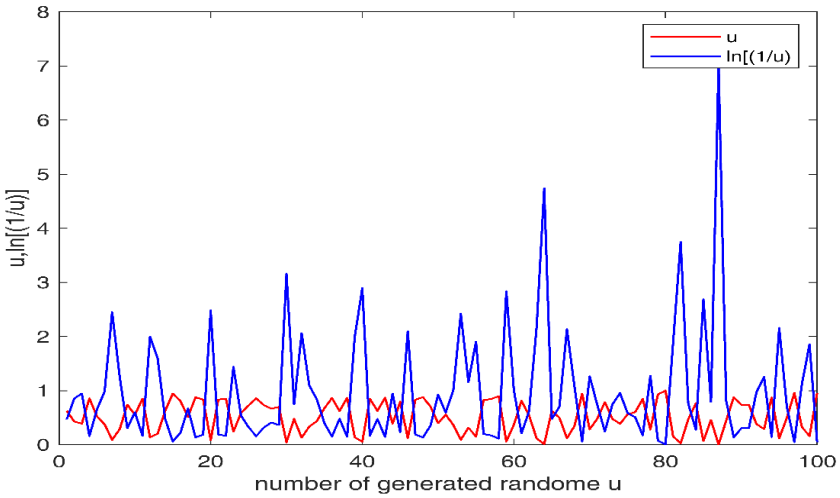

Figure 8. Changes of $\ln(\frac{1}{u})$ for 100 randomly generated numbers of u

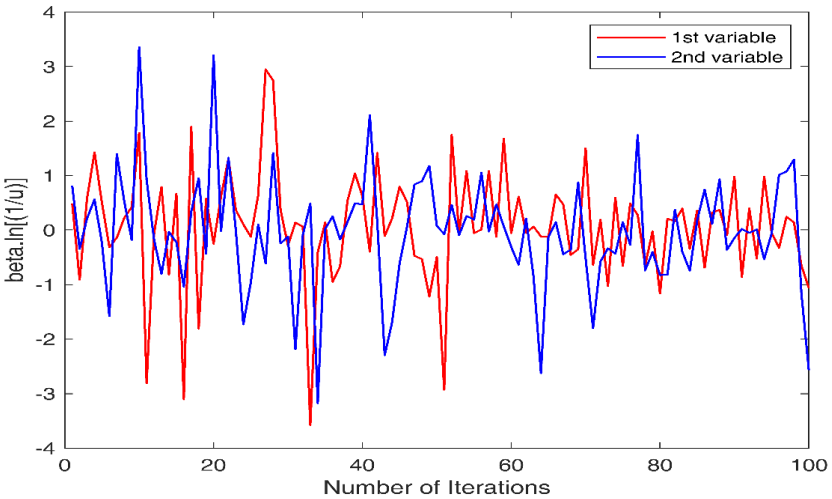

Figure 9. Dynamic of $\pm\beta.\ln(\frac{1}{u})$ for a two-dimensional assumed problem in 100 iterations

The schematic representations of Eq. (29) are shown in Figs. 10 and 11. As mentioned

above, the broad probable region of QTLBO in Figs. 10 and 11, due to the distinct formulation of quantum behaved particle, remarkably explores all solution domains and helps to escape from local optimum and find a robust solution. The steps of the QTLBO method are as follows:

Step one (Initialization): Same as the TLBO algorithm, the initial candidate solutions can be considered as a class with nS students. The set of students (S) can be produced through the following equation:

$$S = Lb + (Ub - Lb) \times rand(nS, nVar) \tag{32}$$

where nS is the number of students, $nVar$ is the number of design variables, and Lb and Ub are the lower and upper bound vectors of the design variables.

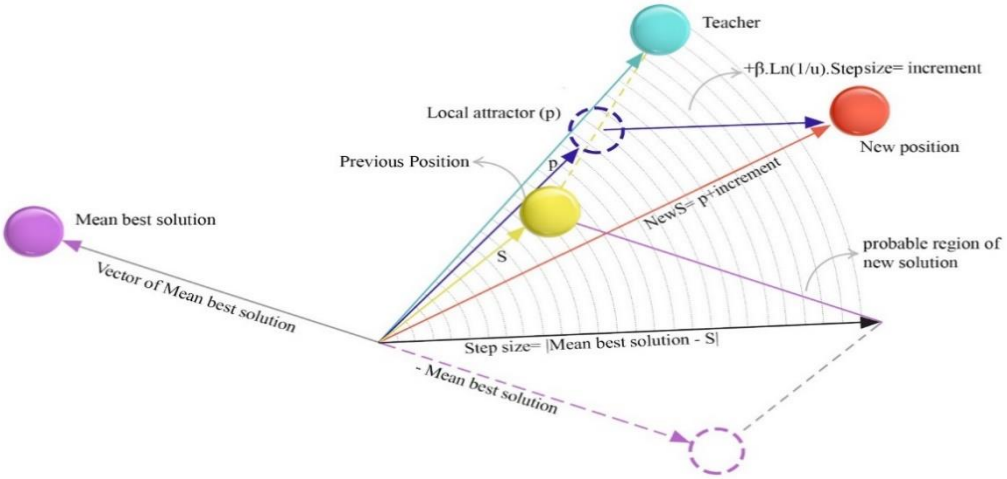

Figure 10. A schematic of generating a new position in the QTLBO using $({x_i}^{new} = p + \beta . \left| p_{mean} - {x_i}^{old} \right| . \ln(\frac{1}{u}))$ at the teacher phase

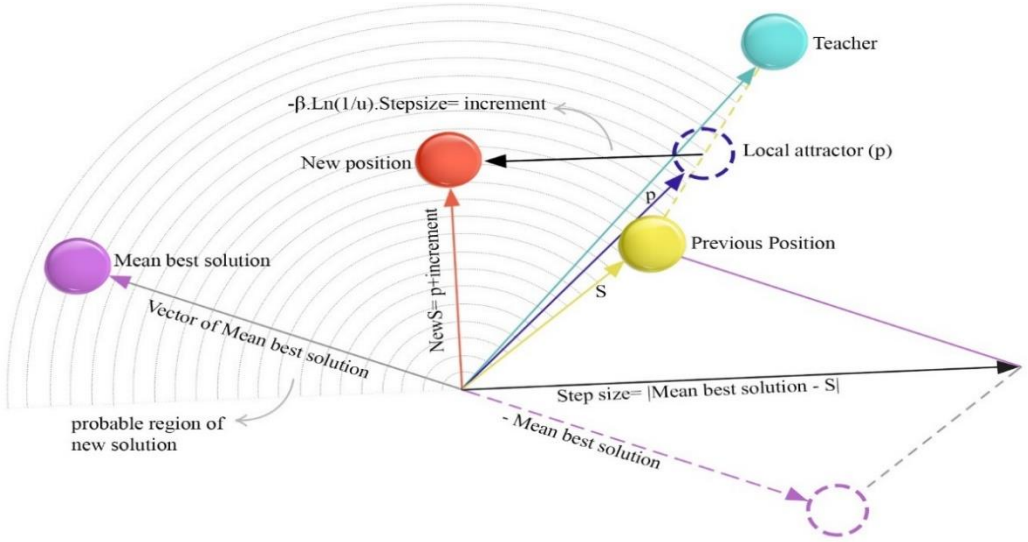

Figure 11. A schematic of generating a new position in the QTLBO using $(x_i^{new} = p - \beta.\left|p_{mean} - x_i^{old}\right|.\ln(\frac{1}{u}))$ at the teacher phase

Step two (quantum teacher phase): After the students' evaluation, their corresponding penalized objective function vector (PFit) is generated. After that, the best student (the student with the best-penalized objective function value) is chosen as the quantum teacher (T). A quantum step size updates the students toward their quantum teacher. The step size is obtained based on the difference between the quantum teacher and the mean solution of all other students (Ave_S). The teacher phase can be formulated as follows:

$$stepsize_i = |Ave_S - S| \times \beta \tag{33}$$

$$newS = p + \ln(\frac{1}{rand()}) \times stepsize \tag{34}$$

$$p = \frac{(c_1.S + c_2.T)}{c_1 + c_2} \; ; \; c_1, c_2 = rand() \tag{35}$$

where $stepsize_i$ is the step size of i-th student, and $newS$ is the vector of new students. Also, the parameters of c_1, c_2, and $rand()$ are random numbers chosen from the interval of [0, 1]. New solutions are always established between a particle and the best one formed in the teacher phase to provide local changes for each particle and a high probability of improving the fitness value. It is assumed that A parameter like $Pro = 0.3$ is introduced to control whether each solution's component must be changed or not. The formulation of this mechanism is as follows:

$$S_{new} = \begin{cases} T + \left(1 - \left(\frac{iter}{iter_{max}}\right)^{\frac{1}{6}}\right) * \left(Lb + rand.(Ub - Lb)\right); r_1 \le 0.3,\ r_2 \le 0.5 \\ T - \left(1 - \left(\frac{iter}{iter_{max}}\right)^{\frac{1}{6}}\right) * \left(Lb + rand.(Ub - Lb)\right); r_1 \le 0.3,\ r_2 \ge 0.5 \\ S_{old}; \qquad r_1 > 0.3 \\ r_1, r_2, \text{and } r_3 \text{ are random numbers in range of } [0,\ 1] \end{cases} \tag{36}$$

Step three (replacement strategy): In this step, newly generated students are evaluated and replaced with their corresponding old ones in a simple greedy manner. In this way, the newly generated student with a better penalized objective function value is preferred to his corresponding old one. Therefore, a new class with nS students is formed.

Step four (learner phase): The learner phase is performed similar to TLBO.

Step five (replacement strategy): The replacement strategy is performed again.

Step six (termination criteria): If the termination criterion of the algorithm is satisfied, the algorithm is terminated. Otherwise, go to step two. The pseudo-code of the QTLBO algorithm is provided in Fig. 12.

Initialization:
Set the algorithm parameters: *nS*, *MaxNFEs*.
Generate random initial candidate solutions or elements (*S*).
Evaluate the set of elements (candidate solutions).
$i = 0$; $NFEs = 0$;
Cyclic body of the algorithm:
While *NFEs < MaxNFEs/k or termination criteria is satisfied*
Step 1: Generate the new solutions (*newS*) based on the quantum teacher phase EQ.(31 to 35).
Step 2: Evaluate the newly generated solutions (*newS*) and apply replacement strategy between old and new candidates.
Update the number of function evaluations ($NFEs = NFEs + nS$).
Step 3: Generate the new solutions (*newS*) based on the learner phase. EQ.(3).
Step 4: Evaluate the newly generated subsets (*newS*) and apply replacement strategy between old and new ones.
Update the number of function evaluations ($NFEs = NFEs + nS$).
Step 5: Monitor the best element found by the TLBO algorithm so far.
EndWhile

Figure 12. The pseudo-code of the QTLBO

2.4 Mathematical formulation of the optimization problem

In a truss sizing optimization problem with frequency constraints, the aim is to minimize the total weight of the structure while satisfying some constraints on natural vibration frequencies. The cross-sectional areas of structural members are considered as continuous design variables. Furthermore, the layout of the structure is pre-defined and kept unchanged during the optimization process. The mathematical formulation of the optimization problem

is as follows [54]:

$$\text{Find: } \{X\} = [x_1, x_2, \dots, x_m] \tag{37}$$

$$\text{to minimize: } P(\{X\}) = f(\{X\}) \times f_{penalty}(\{X\}) \tag{38}$$

$$\text{subject to: } \begin{cases} \omega_j \geq \omega_j^* \text{ for some natural vibration frequencies } j \\ \omega_k \leq \omega_k^* \text{ for some natural vibration frequencies } k \\ L_{b,i} \leq x_i \leq U_{b,i};\ i = 1,2, \dots, m \end{cases} \tag{39}$$

where $\{X\}$ denotes the vector of design variables, including sizing design variables, m is the number of design variables, which is selected considering the member-grouping configuration, x_i is the cross-sectional area of the structural members of the i-th member group, $f(\{X\})$ is the objective function of the optimization problem to be minimized, which represents the total weight of the structure in a weight minimization problem, $f_{penalty}(\{X\})$ is the penalty function which is used to handle the problem constraints, and $P(\{X\})$ is the penalized objective function, $L_{b,i}$ and $U_{b,i}$ are the lower and upper bounds of the crosssectional area of the structural members of the i-th member group, respectively, ω_j and ω_k are the j-th and the k-th natural vibration frequencies of the structure, respectively, ω_j^* is the lower bound of the j-th natural vibration frequency of the structure, and ω_k^* is the upper bound of the k-th natural vibration frequency of the structure. The objective function is considered to be the total weight of the structure and can be defined as follows:

$$f(\{X\}) = W(\{X\}) = \sum_{i=1}^{nE} \rho_i \times A_i \times L_i \tag{40}$$

where ρ_i, A_i, and L_i are the material density, cross-sectional area, and length of the i-the structural member, respectively, nE is the number of structural members of the structure, and $W(\{X\})$ is the total weight of the structure. Various strategies have been suggested to handle constraints in optimization problems, one of the most popular of which is penalizing strategies. The main idea of penalizing strategies is to transform a constrained optimization problem into an unconstrained one by penalizing the infeasible solution and extending an unconstrained objective function [55]. Here, a dynamic penalty function is used to tackle the violated constraints [56]:

$$f_{penalty}(X) = (1 + \varepsilon_1 \times \upsilon)^{\varepsilon_2}, \qquad \upsilon = \sum_{i=1}^{nC} \upsilon_i \tag{41}$$

where nC is the number of constraints of the problem, ε_1 and ε_2 are the penalty parameters that affect the severity of violated constraints, and υ denotes the sum of the constraint violations. The value of υ_i is set to zero if the i-th constraint is satisfied, while in the case of a violated constraint, it is selected considering the severity of the violation. The mathematical expression of υ_i is as follows:

$$v_i = \begin{cases} \left|1 - \dfrac{\omega_i}{\omega_i^*}\right| & \text{if the } i-\text{th frequency constraint is violated} \\ 0 & \text{otherwise} \end{cases} \tag{42}$$

Dynamic penalty functions take into account the progress of the optimization process so that penalty is imposed at a dynamic or increasing rate [55]. This means that a low degree of penalty is imposed at the beginning of the search process. However, as the search process progresses, the degree of the penalty also gradually increases [57]. Such a dynamic strategy encourages the diversification in the search space (i.e., more exploration) in the early iterations of the optimization process, but more emphasis on the intensification of the best solutions found (i.e., more exploitation) in the last iterations [38]. The parameters ε_1 and ε_2 control how much an infeasible solution is penalized. The severity of penalizing is very sensitive to these parameters. Hence, setting the parameters ε_1 and ε_2 is a challenging task and requires many preliminary trials [58]. Indeed, if they are chosen too small, feasible regions of search space may not be explored effectively, and even the algorithm may never converge toward a feasible solution. On the other hand, if they are too large, premature convergence may occur [59]. In this study, a constant value for the parameter ε_1 is chosen, whereas the parameter ε_2 increases monotonically with the number of iterations.

3. RESULTS AND DISCUSSION

3.1 Numerical examples

Two well-known dome structure optimization problems with multiple frequency constraints are considered from the literature to assess the developed algorithm's performance. The optimization problems are as follows: (a) size optimization of a 600-bar dome truss with 25 design variables; and (b) size optimization of a 1180-bar dome truss with 59 design variables. For each mentioned problem, the QTLBO algorithm results are compared with those of TLBO and other optimization algorithms in the literature. Convergence histories of the problems are provided, and an over-scaled part is attached to each convergence curve to display curves well. Also, optimized results at different stages of the optimization process are provided for each problem, which allows comparing the algorithms' performance. Ten independent runs have been executed to achieve a fair comparison of the algorithms' performance, and the results of the best ones have been reported. For all runs, the initial population is generated randomly. The maximum number of objective function evaluations ($MaxNFEs$) is considered as the stopping criterion of the algorithm.

3.1.1 A 600-bar dome truss

Figure 13 schematically shows the structure of a 600 bars single-layer dome. The whole structure consists of 216 nodes and 600 elements. Figure 14 shows the typical sub-structure in more detail about how the nodes are numbered. Table 1 lists the nodal coordinates of the typical sub-structure in the Cartesian coordinate system. Each element of this sub-structure is considered a design variable. Therefore, the problem of the 600-bar dome is an

optimization problem with 25 design variables. The modulus of elasticity is 200 GPa, and the material density is 7850 kg/ m^3 for all elements. A non-structural mass of 100 kg it attached to all free nodes as lumped mass. All elements' minimum and maximum allowable area of cross-sections are assumed to be 1 and 100 cm^2, respectively. In the present problem, two frequency constraints are considered, $\omega_1 \geq 5$ Hz and $\omega_3 \geq 7$ Hz, which are related to the first and third modes of the structure in free vibration analysis.

Kaveh et al. [62] proposed a formulation to swiftly solve characteristic equations obtained from free vibration of the circulant symmetric structures based on optimal analysis and graph theory. In the cylindrical coordinate system, the structural matrices corresponding to a cyclic symmetric structure exhibit a unique pattern known as block circulant [22]. Circulant matrices can be expressed as the sum of Kronecker products in which the first components satisfy the commutative property of multiplication [51]. This property facilitates the block diagonalization of circulant matrices. Therefore, using this property of block circulant matrices, the initial generalized eigenvalue problem, derived from the free vibration analysis, is decomposed into highly smaller sub-eigenproblems [53]. This approach leads to the high accuracy of the free vibration analysis results and a significant decrease in computational time and memory usage compared to the existing classical eigenvalue solutions [22]. However, the present block-diagonalization technique is suitable only for cyclic symmetric configurations.

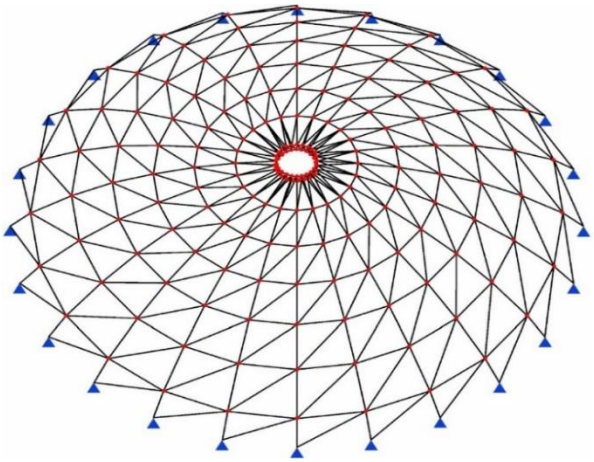

Figure 13. The 600-bar single-layer dome

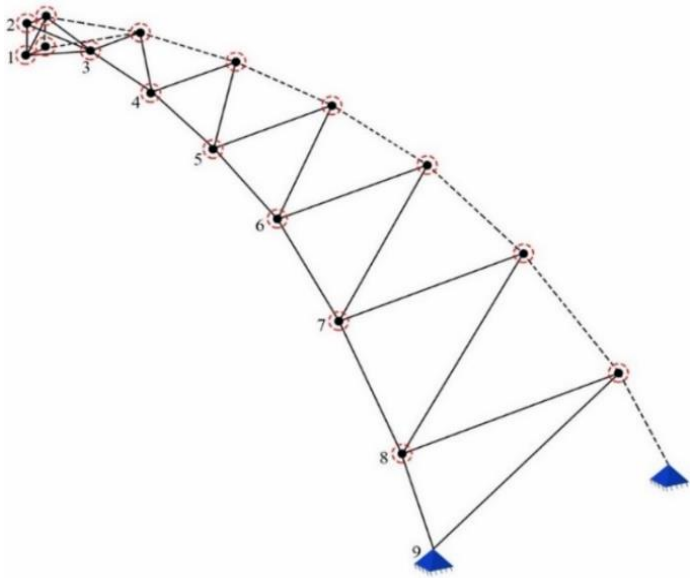

Figure 14. Details of a sub-structure of the 600-bar single-layer dome

Table 2 shows the optimal results obtained from different methods in the literature on the 600-bar dome truss problem and the results of current and quantum versions of TLBO methods. Table 3 shows the frequency values at the first five-mode of 600 bars dome. A quick look at Table 2 shows that the improved method with the quantum framework has an acceptable comparative optimal solution compared to the minimum results in Table 2 in 10 consecutive runs. The main reason is to utilize the quantum teacher with a better exploration rate in the last iterations than using the classical version of TLBO. The minimum optimal solution without violating the problem constraints is 6063.59 kg, related to the QTLBO method.

Meanwhile, according to the results given in Table 2, the obtained optimal solution so far is 6065.811 kg related to the ST-JA method. Although the least optimal weight of the TLBO and QTLBO are approximately close, the worst and standard deviations obtained by QTLBO are remarkably more minor than those of the TLBO method. Regarding the performance improvement in Table 2, the statistical results section for the standard deviation and the worst response based on quantum behaved particles significantly reduce the values of statistical indices obtained from 10 consecutive runs.

Figure 15 shows the distributed results obtained from 10 consecutive runs through the TLBO and QTLBO. What can be deduced from these diagrams is that in the quantum version, the solutions are significantly inclined towards the minimum solution. In other words, the solutions are focused on a region between the mean and minimum answers. Considering performance, Fig. 15 compares TLBO and QTLBO methods in ten consecutive runs and shows that the QTLBO method efficiently improves the classic version of TLBO to find a better performance. The value of penalized weight in the worst solution obtained with the QTLBO is much better and less than the conventional methods of TLBO, leading to a reduced standard deviation index and coefficient of variation

The above performance causes that in Fig. 16 showing the history diagrams obtained from the average of 10 consecutive performances, the QTLBO gives better results than the

conventional TLBO during objective function evaluations. As shown in Table 3, none of the optimal obtained solutions violates the constraint. Results show that QTLBO could exhibit a better exploration than TLBO without any redundant parameter tuning.

Table 1: Coordinates of the nodes of the 600-bar dome-like truss

Node number	Coordinates (x, y, z) (m)
1	(1.0, 0.0, 7.0)
2	(1.0, 0.0, 7.5)
3	(3.0, 0.0, 7.25)
4	(5.0, 0.0, 6.75)
5	(7.0, 0.0, 6.0)
6	(9.0, 0.0, 5.0)
7	(11.0, 0.0, 3.5)
8	(13.0, 0.0, 1.5)
9	(14.0, 0.0, 0.0)

Table 2: Comparison results of TLBO and QTLBO methods for the 600-bar dome truss with different methods of literature (cm^2)

Element number (element nodes)	ECBO-Cascade [60]	CBO [61]	MDVC-UPVS [62]	PFJA [63]	JA [64]	ST-JA [64]	This study	
							TLBO	QTLBO
1 (1-2)	1.0299	1.2404	1.2575	1.1867	1.0703	1.3964	1.0634	1.2371
2 (1-3)	1.3664	1.3797	1.3466	1.2967	1.2699	1.5177	1.5201	1.3390
3 (1-10)	5.1095	5.2597	4.9738	4.5771	4.0174	5.5370	5.2091	5.0958
4 (1-11)	1.3011	1.2658	1.4025	1.3356	1.0036	1.2549	1.3610	1.3948
5 (2-3)	17.0572	17.2255	17.3802	18.3157	16.9565	16.7759	17.0588	16.8895
6 (2-11)	34.0764	38.2991	37.9742	38.5097	39.2560	36.8528	36.7938	38.7177
7 (3-4)	13.0985	12.2234	13.0306	13.5917	13.2920	12.8198	12.4260	12.7778
8 (3-11)	15.5882	15.4712	15.9209	16.8824	15.1664	15.4141	15.2655	15.8387
9 (3-12)	12.6889	11.1577	11.9419	13.8766	10.8041	12.0638	12.2102	11.5202
10 (4-5)	10.3314	9.4636	9.1643	9.5286	8.9660	9.3500	9.3867	9.2533
11 (4-12)	8.5313	8.8250	8.4332	9.4218	8.7332	8.2980	8.3280	8.2397
12 (4-13)	9.8308	9.1021	9.2375	9.7643	8.8557	8.8205	8.7327	9.6497
13 (5-6)	7.0101	6.8417	7.2213	7.2431	7.7360	7.4253	7.1844	7.2848
14 (5-13)	5.2917	5.2882	5.2142	5.3913	5.1991	5.1621	5.0898	4.9730
15 (5-14)	6.2750	6.7702	6.7961	6.7468	6.5265	6.6351	6.7874	6.4594
16 (6-7)	5.4305	5.1402	5.2078	5.1493	5.1082	4.9351	5.3090	5.0868
17 (6-14)	3.6414	5.1827	3.4586	3.8342	3.7784	3.5639	3.9638	3.5197
18 (6-15)	7.2827	7.4781	7.6407	8.0665	7.8962	8.0435	7.3660	7.7938
19 (7-8)	4.4912	4.5646	4.3690	4.2800	4.0664	4.2061	4.5322	4.3793
20 (7-15)	1.9275	1.8617	2.1237	2.2509	2.3832	2.3310	2.1173	2.1781
21 (7-16)	4.6958	4.8797	4.5774	4.5372	4.9196	4.4953	4.5101	4.3913
22 (8-9)	3.3595	3.5065	3.4564	3.5615	3.1955	3.4287	3.6624	3.6701

23 (8-16)	1.7067	2.4546	1.7920	1.7744	1.9531	1.8660	2.0548	1.8443
24 (8-17)	4.8372	4.9128	4.8264	4.6445	4.7961	4.9318	4.9345	4.7175
25 (9-17)	2.0253	1.2324	1.7601	1.6141	1.3999	1.5022	1.3931	1.6930
The Best weight (kg)	6140.51	6182.01	6115.10	6333.251	6082.889	6065.811	6075.15	6063.59
Average weight (kg)	6175.33	6226.37	6119.95	6380.31	6090.345	6072.734	6457.10	6072.31
The worst weight (kg)	N/A	N/A	N/A	N/A	6101.777	6084.749	7798.94	6081.48
Standard deviation (kg)	34.08	60.12	16.23	47.396	6.455	6.182	637.95	5.00
Maximum number of FE analyses	20,000	20,000	18,000	25,000	12,000	12,000	20,000	20,000

Table 3: Natural frequencies (Hz) of the optimal designs for the 600-bar dome

Frequency number	ECBO-Cascade [60]	CBO [61]	MDVC-UPVS [62]	PFJA [63]	JA [64]	ST-JA [64]	This study	
							TLBO	QTLBO
1	5.001	5.000	5.000	5.0011	5.0052	5.0002	5.0035	5.0016
2	5.001	5.000	5.000	5.0011	5.0052	5.0002	5.0035	5.0016
3	7.001	7.000	7.000	7.0000	7.0002	7.0002	7.0002	7.000
4	7.001	7.000	7.000	7.0000	7.0009	7.0006	7.0002	7.000
5	7.002	7.001	7.000	7.0000	7.0009	7.0006	7.0015	7.000

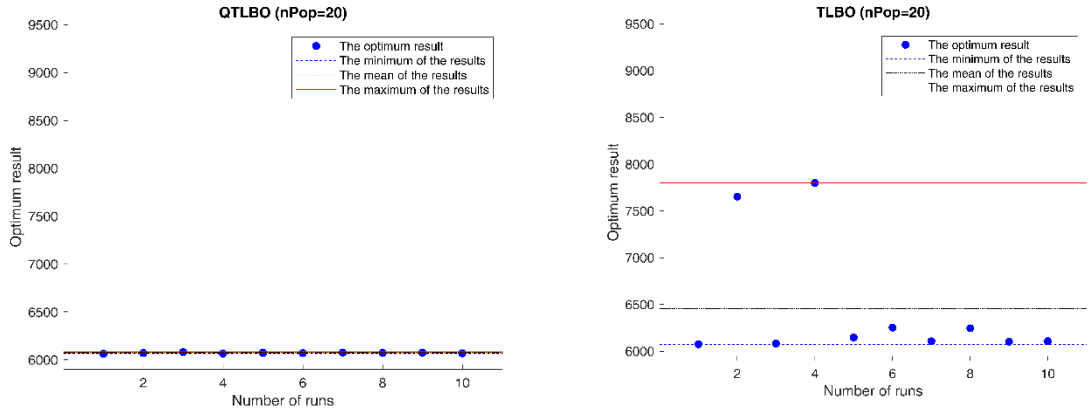

Figure 15. Comparison of the obtained structural weight in each independent run for the 600-bar dome

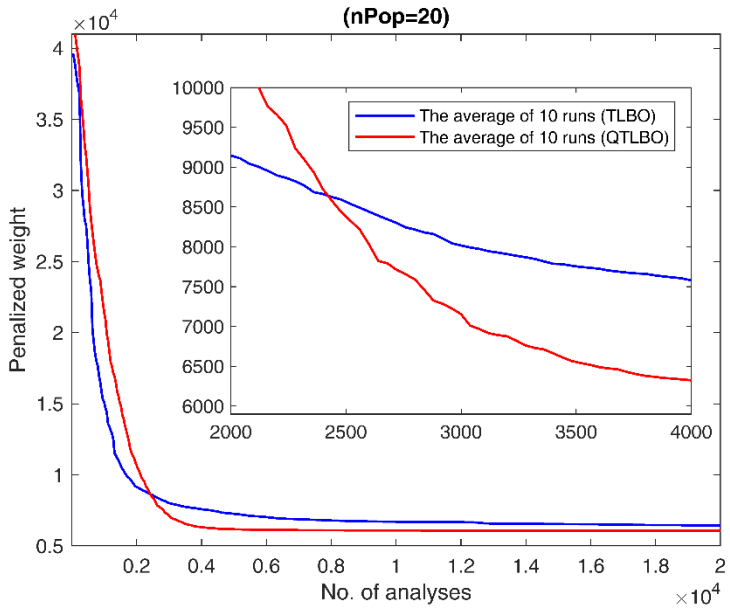

Figure 16. Convergence history of the TLBO and QTLBO for the 600-bar dome (average of 10 runs) ($NP = 20$)

3.1.2 A 1180-bar dome truss

The optimization problem of the 1180 bar dome truss is another example to evaluate the performance of the QTLBO method. Figure 17 depicts the schematic of the structure. This structure consists of 400 nodes and 1180 structural members. This dome's generating sub-structure is shown in Fig. 18 in more detail for numbering nodes. Each element of this sub-structure is considered a design variable. Therefore, the 1180 dome truss structure is an optimization problem with 59 design variables. Table 4 shows the coordinates of nodes in a Cartesian coordinate system. In this case, the modulus of elasticity is 200 GPa, and the material density is 7850 kg/m^3 for all elements. A non-structural mass of 100 kg is attached to all free nodes of the dome.

All elements' minimum and maximum allowable area of cross-sections are assumed to be 1 and 100 cm^2, respectively. In the present problem, two frequency constraints are considered, $\omega_1 \geq 7$ Hz and $\omega_3 \geq 9$ Hz, which are related to the first and third modes of the structure in free vibration analysis.

Due to the usage of quantum-behaved particles features in QTLBO, remarkable results have been obtained, like another case study mentioned in this paper. Accessing convenient optimal minimum values, which are better than those of the TLBO algorithm and some methods in the literature shown in Table 5, is one of the advantages of using a quantum framework. This framework provides accessing better solutions meanwhile searching more efficiently with appropriate convergence rates. In addition, other statistical indices such as mean and the worst solution have significantly improved besides standard deviation. The results of the current and quantum versions of the TLBO are given in Table 5. Table 6 shows the frequency values of the first to fifth free vibration modes of the 1180 bar dome, in which there is no violation of the constraints.

Figure 19 shows the results obtained from 10 consecutive runs for the TLBO algorithms and their quantum version. As mentioned in the study of the results in Table 5, we expected the quantum version to provide better search capability and reduce the standard deviation by a reasonable amount, which is seen in the quality of the algorithm distributed results in the above figures. The inclination of the solution towards the least optimal answer and the significant weight reduction of the worst solution is a good help in detecting the practical improvement of the algorithms. Figure 20 shows the history diagram obtained from the average results of 10 consecutive independent runs. The average weight values obtained from the quantum version in all algorithm iterations are less than the current version of TLBO.

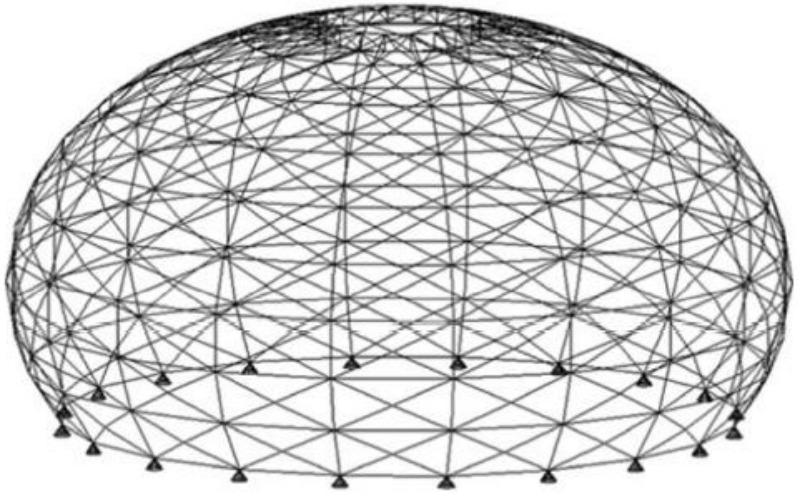

Figure 17. The 1180-bar single-layer dome

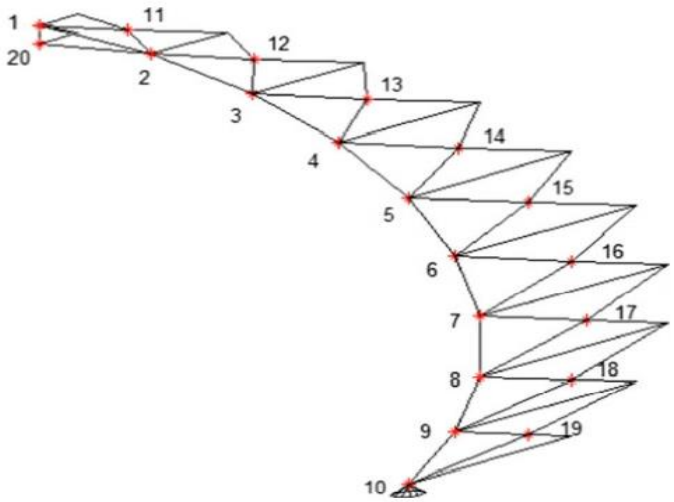

Figure 18. Details of a sub-structure of the 1180-bar single-layer dome

Table 4: Coordinates of the nodes of the 1180-bar dome-like truss

Node number	Coordinates (x, y, z) (m)	Node number	Coordinates (x, y, z) (m)
1	(3.1181, 0.0, 14.6723)	11	(4.5788, 0.7252, 14.2657)
2	(6.1013, 0.0, 13.7031)	12	(7.4077, 1.1733, 12.9904)
3	(8.8166, 0.0, 12.1354)	13	(9.9130, 1.5701, 11.1476)
4	(11.1476, 0.0, 10.0365)	14	(11.9860, 1.8984, 8.8165)
5	(12.9904, 0.0, 7.5000)	15	(13.5344, 2.1436, 6.1013)
6	(14.2657, 0.0, 4.6358)	16	(14.4917, 2.2953, 3.1180)
7	(14.9179, 0.0, 1.5676)	17	(14.8153, 2.3465, 0.0)
8	(14.9179, 0.0, -1.5677)	18	(14.9179, 2.2953, -3.1181)
9	(14.2656, 0.0, -4.6359)	19	(13.5343, 2.1436, -6.1014)
10	(12.9903, 0.0, -7.5001)	20	(3.1181, 0.0, 13.7031)

Table 5: Comparison results of TLBO and QTLBO methods for the 1180-bar dome truss with different methods of literature (cm^2)

Element number (element nodes)	CBO [61]	ECBO [61]	VPS [62]	MDVC-UPVS [62]	This study	
					TLBO	QTLBO
1 (1-2)	13.0171	7.6678	6.8743	7.3691	6.2075	6.8443
2 (1-11)	10.4346	11.1437	10.0230	9.3399	9.8913	9.8186
3 (1-20)	3.0726	1.8520	4.4140	2.7203	2.0235	3.4713
4 (1-21)	12.6969	14.5563	13.5515	13.2822	15.4007	13.9640
5 (1-40)	3.5654	4.9499	1.8303	3.6758	5.3031	4.0370
6 (2-3)	6.5190	6.8095	7.0824	6.1391	6.4202	6.1996
7 (2-11)	7.4233	6.6803	6.3960	7.0964	6.7999	7.5473
8 (2-12)	6.3471	6.7889	6.5646	6.0208	3.8638	6.0971
9 (2-20)	2.3013	1.0630	2.3705	2.1225	3.9379	1.3435
10 (2-22)	12.1936	9.1602	13.2621	12.3488	11.5361	12.1911
11 (3-4)	7.2877	6.9891	7.0922	6.8578	9.6721	7.3537
12 (3-12)	7.0961	6.9881	6.8079	5.7773	5.2983	5.6248
13 (3-13)	6.5669	6.9555	6.3815	6.9931	4.7727	6.8738
14 (3-23)	7.8257	7.5443	7.3122	7.3355	12.6813	6.4318
15 (4-5)	8.6812	9.5431	8.7221	10.5464	8.4290	9.5515
16 (4-13)	5.7888	6.9123	6.3680	6.9589	6.4138	6.7510
17 (4-14)	21.1342	8.9891	7.3159	8.0977	8.9110	7.7054
18 (4-24)	10.0502	6.8926	11.5749	7.7738	7.1333	7.8099
19 (5-6)	12.9279	12.6128	14.7985	12.4614	10.9557	12.2147
20 (5-14)	9.3212	8.1983	5.5174	7.8154	10.3955	8.1532
21 (5-15)	10.1260	11.8358	15.7381	10.2039	54.5223	10.7008
22 (5-25)	10.1358	9.7321	8.3419	8.9262	7.7235	9.1762
23 (6-7)	15.8585	19.1650	17.5000	16.5275	16.1223	16.7267
24 (6-15)	9.9672	10.4682	10.3084	9.0166	10.6541	11.0430
25 (6-16)	14.8493	14.1178	15.1958	13.8204	13.6736	12.7295
26 (6-26)	11.4909	11.14567	10.9395	11.4021	12.8061	11.9334

27 (7-8)	26.2359	23.4125	24.9421	24.2631	25.9787	24.6152
28 (7-16)	13.8812	15.5167	13.9614	14.5494	11.8588	13.4045
29 (7-17)	18.8857	16.6613	18.4153	17.7753	44.7192	19.0138
30 (7-27)	14.0257	15.9631	14.4945	15.4594	12.1242	15.9277
31 (8-9)	33.8826	37.0532	36.3529	34.1372	38.9405	34.8418
32 (8-17)	25.7142	22.2937	19.6608	19.1254	15.2119	21.4674
33 (8-18)	24.8644	22.7409	23.7259	24.1954	23.5875	22.1760
34 (8-28)	19.8498	23.5624	22.0297	21.5899	35.1567	21.3054
35 (9-10)	53.2630	47.7652	47.3286	49.4717	44.3518	48.1875
36 (9-18)	22.7771	22.5066	22.9442	26.2915	27.4562	22.6174
37 (9-19)	35.4230	34.6418	30.8229	33.7558	48.1280	34.3705
38 (9-29)	57.5480	31.6492	33.1098	29.7608	33.9007	33.2805
39 (10-19)	35.1385	32.7268	32.5526	34.0489	30.8445	35.2950
40 (10-30)	10.7300	1.05206	1.7363	1.0024	1.0001	1.0331
41 (11-21)	9.2401	11.3681	11.5271	9.0344	10.3408	9.8014
42 (11-22)	5.2661	6.5512	8.4571	7.5316	7.1571	7.1106
43 (12-22)	6.2415	6.3619	5.4136	6.3726	7.1878	6.3135
44 (12-23)	4.4768	5.9296	7.1832	5.7643	5.8172	6.3825
45 (13-23)	8.8846	7.8739	5.4066	6.7270	10.9891	7.1512
46 (13-24)	7.3710	6.2794	6.2534	6.7021	7.5391	6.6035
47 (14-24)	8.2595	7.6206	6.9383	7.8082	7.2565	8.7801
48 (14-25)	7.6091	7.2937	10.6872	8.1225	8.7307	9.0923
49 (15-25)	11.3030	10.5783	12.8005	10.1777	9.2994	11.8150
50 (15-26)	13.8381	10.1173	10.2216	10.1825	9.4147	10.1750
51 (16-26)	13.3654	15.1088	11.5330	13.4590	29.5867	12.8583
52 (16-27)	13.1836	12.8251	11.6918	13.9788	14.1291	14.4375
53 (17-27)	13.5793	17.4375	20.7566	18.1070	11.8872	17.1922
54 (17-28)	10.0628	20.1153	18.1341	19.2212	26.4427	18.7209
55 (18-28)	24.1197	24.2121	28.2882	23.4359	22.9082	25.5041
56 (18-29)	24.2604	23.3175	24.2023	27.6479	21.8279	27.8431
57 (19-29)	34.1389	34.6196	48.0180	33.6805	36.4962	29.3963
58 (19-30)	38.0340	35.2970	35.6517	35.7035	67.0118	32.7544
59 (20-40)	2.6689	8.8569	5.5956	4.7617	4.8047	5.3197
The Best weight (kg)	40,985	37,984.39	38,699.14	37,451.77	44084.90	37579.57
Average weight (kg)	42,019.10	38,042.15	38,861.82	37,545.53	49329.31	37817.94
The worst weight (kg)	N/A	N/A	N/A	N/A	54768.63	38002.71
Standard deviation (kg)	655.72	101.43	385.41	64.85	3005.51	150.28
Maximum number of FE analyses	9000	30,000	20,000	20,000	20,000	20,000

Table 6: Natural frequencies (Hz) of the optimal designs for the 1180-bar dome

Frequency number	CBO [61]	ECBO [61]	VPS [62]	MDVC-UPVS [62]	This study	
					TLBO	QTLBO

1	7.0017	7.0017	7.0019	7.0019	7.0041	7.000
2	7.0017	7.0017	7.0019	7.0019	7.0041	7.000
3	9.0141	9.0259	9.0289	9.0124	9.0065	9.0039
4	9.0188	9.0259	9.0289	9.0251	9.0065	9.0039
5	9.0188	9.071	9.1846	9.0251	9.2832	9.007

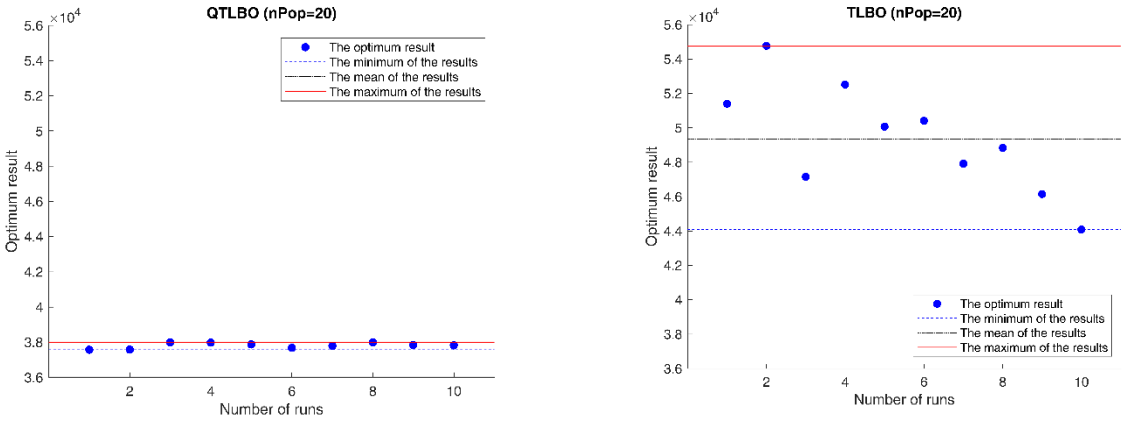

Figure 19. Comparison of the obtained structural weight in each independent run for the 1180-bar dome

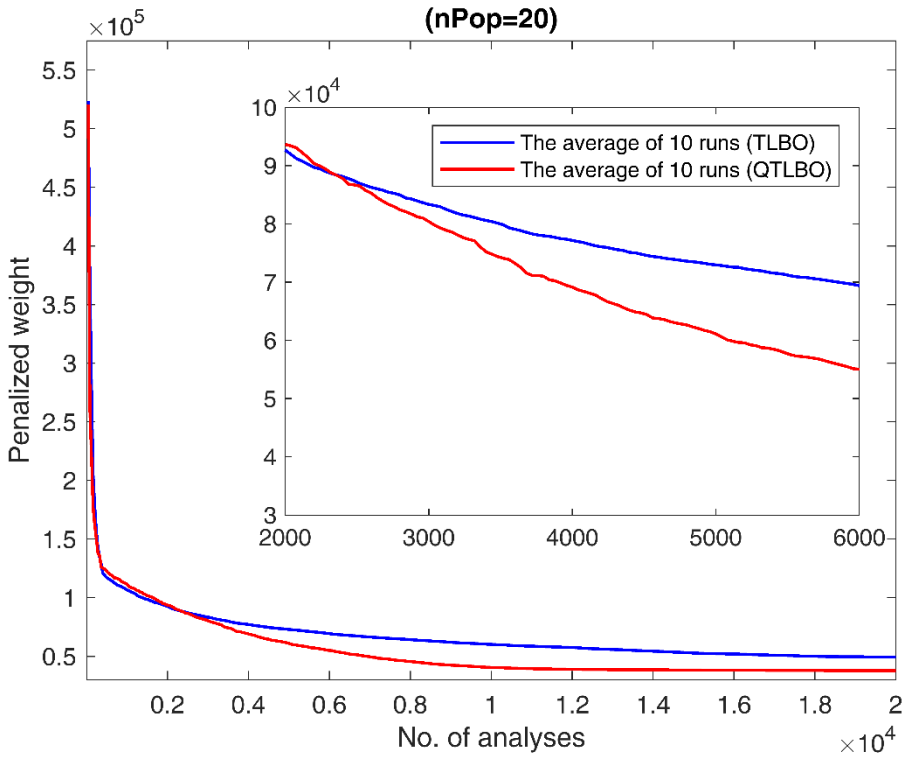

Figure 20. Convergence history of the TLBO and QTLBO for the 1180-bar dome (average of 10

runs) ($NP = 20$)

4. CONCLUSION

In this paper, the Quantum Teaching-Learning-Based Optimization (QTLBO) is evaluated by optimizing the 600-bar and 1180-bar domes with multiple frequency constraints to improve the performance of TLBO. In QTLBO, the teacher phase was redefined using the quantum framework. A particular formulation was obtained from solving the time-independent Schrodinger differential equation in the delta-potential-well function to update the solution candidates' positions. Although QTLBO has a simple formulation and requires no internal parameter tuning similar to the former version of TLBO, it establishes the right balance between local and global search phases to escape from a local minimum in some NP-hard problems. In the teacher phase of QTLBO, the local attractors as possible solutions between the best solution and the others are introduced to explore the solution space. Both local attractors and new step size definition from the quantum framework guarantee diversification besides the inherent intensification. Results show that QTLBO outperforms the former version of TLBO and increases the chance of finding a better solution besides improving the statistical criteria compared to the current TLBO. Conclusively, using quantum-behaved particles could be a successful strategy to improve optimization algorithms' performance. Finally, The quantum framework could be implemented by changing a part of an algorithm like QTLBO or hybridizing with a particular optimization method like QECBO.

Declaration of Competing Interest: The authors declare that they have no known competing financial interests or personal relationships that could have appeared to influence the work reported in this paper.

REFERENCES

1. Holland JH. *Adaptation in natural and artificial systems: an introductory analysis with applications to biology, control, and artificial intelligence*, MIT Press, 1992.
2. Dorigo M, Birattari M, Stutzle T. Ant colony optimization, *IEEE Comput Intell Mag* 2006; **1**(4): 28-39. https://doi.org/10.1109/MCI.2006.329691
3. Kennedy J, Eberhart R. Particle swarm optimization. InProceedings of ICNN'95-international conference on neural networks 1995 (Vol. **4**, pp. 1942-1948). IEEE. https://doi.org/10.1109/ICNN.1995.488968
4. Kirkpatrick S, Gelatt Jr CD, Vecchi MP. Optimization by simulated annealing, *Science* 1983; **220**(4598): 671-80. https://doi.org/10.1126/science.220.4598.671
5. Duan QY, Gupta VK, Sorooshian S. Shuffled complex evolution approach for effective and efficient global minimization, *J Optim Theory Appl* 1993; **76**(3): 501-21. https://doi.org/10.1007/BF00939380
6. Karaboga D. An idea based on honey bee swarm for numerical optimization. Technical report-tr06, Erciyes university, engineering faculty, computer engineering department; 2005 Oct.

7. Eusuff M, Lansey K, Pasha F. Shuffled frog-leaping algorithm: a memetic meta-heuristic for discrete optimization, *Eng Optim* 2006; **38**(2): 129-54. https://doi.org/10.1080/03052150500384759
8. Yang XS, Deb S. Cuckoo search via Lévy flights. In2009 World congress on nature & biologically inspired computing (NaBIC) 2009 (pp. 210-214). Ieee. https://doi.org/10.1109/NABIC.2009.5393690
9. Das S, Suganthan PN. Differential evolution: A survey of the state-of-the-art, *IEEE Trans Evol Comput* 2010 ; **15**(1): 4-31. https://doi.org/10.1109/TEVC.2010.2059031
10. Rao RV, Savsani VJ, Vakharia DP. Teaching–learning-based optimization: a novel method for constrained mechanical design optimization problems, *Comput Aid Des* 2011; **43**(3): 303-15. https://doi.org/10.1016/j.cad.2010.12.015
11. Yang XS, Gandomi AH. Bat algorithm: a novel approach for global engineering optimization, *Eng Comput* 2012; **29**(5): 464-83. https://doi.org/10.1108/02644401211235834
12. Mirjalili S, Mirjalili SM, Lewis A. Grey wolf optimizer, *Adv Eng Softw* 2014; **69**: 46-61. https://doi.org/10.1016/j.advengsoft.2013.12.007
13. Wolpert DH, Macready WG. No free lunch theorems for optimization, *IEEE Trans Evol Comput* 1997; **1**(1): 67-82. https://doi.org/10.1109/4235.585893
14. Kaveh A, Talatahari S. A novel heuristic optimization method: charged system search, *Acta Mech* 2010; **213**(3): 267-89. https://doi.org/10.1007/s00707-009-0270-4
15. Kaveh A, Khayatazad M. A new meta-heuristic method: ray optimization, *Comput Struct* 2012; **112**: 283-94. https://doi.org/10.1016/j.compstruc.2012.09.003
16. Kaveh A, Farhoudi N. A new optimization method: Dolphin echolocation, *Adv Eng Softw* 2013; **59**: 53-70. https://doi.org/10.1016/j.advengsoft.2013.03.004
17. Kaveh A, Mahdavi VR. Colliding bodies optimization: a novel meta-heuristic method, *Comput Struct* 2014; **139**: 18-27. https://doi.org/10.1016/j.compstruc.2014.04.005
18. Kaveh A, Bakhshpoori T. Water evaporation optimization: a novel physically inspired optimization algorithm, *Comput Struct* 2016; **167**: 69-85. https://doi.org/10.1016/j.compstruc.2016.01.008
19. Kaveh A, Dadras A. A novel meta-heuristic optimization algorithm: thermal exchange optimization, *Adv Eng Softw* 2017; **110**: 69-84. https://doi.org/10.1016/j.advengsoft.2017.03.014
20. Kaveh A, Dadras Eslamlou A. Water strider algorithm: A new metaheuristic and applications, *Structures* 2020; **25**: 520-41. https://doi.org/10.1016/j.istruc.2020.03.033
21. Kaveh A, Kamalinejad M, Arzani H. Quantum evolutionary algorithm hybridized with Enhanced colliding bodies for optimization, *Structures* 2020; **28**: 1479-501. https://doi.org/10.1016/j.istruc.2020.09.079
22. El Moumen S, Ellaia R, Aboulaich R. A new hybrid method for solving global optimization problem, *Appl Math Comput* 2011; **218**(7): 3265-76. https://doi.org/10.1016/j.amc.2011.08.066
23. Fan SK, Zahara E. A hybrid simplex search and particle swarm optimization for unconstrained optimization, *Eur J Oper Res* 2007; **181**(2): 527-48. https://doi.org/10.1016/j.ejor.2006.06.034
24. Olenšek J, Tuma T, Puhan J, Bűrmen Á. A new asynchronous parallel global optimization method based on simulated annealing and differential evolution, *Appl Soft Comput* 2011; **11**(1): 1481-9. https://doi.org/10.1016/j.asoc.2010.04.019

25. Liu G, Li Y, Nie X, Zheng H. A novel clustering-based differential evolution with 2 multi-parent crossovers for global optimization, *Appl Soft Comput* 2012; **12**(2): 663-81. https://doi.org/10.1016/j.asoc.2011.09.020
26. Cai Z, Gong W, Ling CX, Zhang H. A clustering-based differential evolution for global optimization, *Appl Soft Comput* 2011; **11**(1): 1363-79. https://doi.org/10.1016/j.asoc.2010.04.008
27. Mashinchi MH, Orgun MA, Pedrycz W. Hybrid optimization with improved tabu search, *Appl Soft Comput* 2011; **11**(2): 1993-2006. https://doi.org/10.1016/j.asoc.2010.06.015
28. Li G, Niu P, Xiao X. Development and investigation of efficient artificial bee colony algorithm for numerical function optimization, *Appl Soft Comput* 2012; **12**(1): 320-32. https://doi.org/10.1016/j.asoc.2011.08.040
29. Zhu G, Kwong S. Gbest-guided artificial bee colony algorithm for numerical function optimization, *Appl Math Comput* 2010; **217**(7): 3166-73. https://doi.org/10.1016/j.amc.2010.08.049
30. Akay B, Karaboga D. A modified artificial bee colony algorithm for real-parameter optimization, *Inf Sci* 2012; **192**: 120-42. https://doi.org/10.1016/j.ins.2010.07.015
31. Mahdavi M, Fesanghary M, Damangir E. An improved harmony search algorithm for solving optimization problems, *Appl Math Comput* 2007; **188**(2): 1567-79. https://doi.org/10.1016/j.amc.2006.11.033
32. Lloyd S. Computational capacity of the universe, *Phys Rev Lett* 2002; **88**(23): 237901. https://doi.org/10.1103/PhysRevLett.88.237901
33. He Y, Sun J. Quantum search in structured database. InInternational Conference on Natural Computation 2005 (pp. 434-443). Springer, Berlin, Heidelberg. https://doi.org/10.1007/11539902_52
34. Kamalinejad M, Arzani H, Kaveh A. Quantum evolutionary algorithm with rotational gate and H_{ε}-gate updating in real and integer domains for optimization, *Acta Mech* 2019; **230**(8): 2937-61. https://doi.org/10.1007/s00707-019-02439-2
35. Rao RV, Patel V. Multi-objective optimization of two stage thermoelectric cooler using a modified teaching–learning-based optimization algorithm, *Eng Appl Artif Intell* 2013; **26**(1): 430-45. https://doi.org/10.1016/j.engappai.2012.02.016
36. Črepinšek M, Liu SH, Mernik L. A note on teaching–learning-based optimization algorithm, *Inf Sci* 2012; **212**: 79-93. https://doi.org/10.1016/j.ins.2012.05.009
37. Kaveh A, Kamalinejad M, Hamedani KB, Arzani H. Quantum Teaching-Learning-Based Optimization algorithm for sizing optimization of skeletal structures with discrete variables, *Structures* 2021; **32**: 1798-819. https://doi.org/10.1016/j.istruc.2021.03.046
38. Kaveh A, Zolghadr A. Optimal design of cyclically symmetric trusses with frequency constraints using cyclical parthenogenesis algorithm, *Adv Struct Eng* 2018; **21**(5): 739-55. https://doi.org/10.1177%2F1369433217732492
39. Grandhi R. Structural optimization with frequency constraints-a review, *AIAA J* 1993; **31**(12): 2296-303. https://doi.org/10.2514/3.11928
40. Bellagamba L, Yang TY. Minimum-mass truss structures with constraints on fundamental natural frequency, *AIAA J* 1981; **19**(11): 1452-8. https://doi.org/10.2514/3.7875
41. Grandhi RV, Venkayya VB. Structural optimization with frequency constraints, *AIAA J* 1988; **26**(7): 858-66. https://doi.org/10.2514/3.11928
42. Tong WH, Liu GR. An optimization procedure for truss structures with discrete design variables and dynamic constraints, *Comput Struct* 2001; **79**(2): 155-62. https://doi.org/10.1016/S0045-7949(00)00124-3

43. Sedaghati R, Suleman A, Tabarrok B. Structural optimization with frequency constraints using the finite element force method, *AIAA J* 2002; **40**(2): 382-8. https://doi.org/10.2514/2.1657
44. Lingyun W, Mei Z, Guangming W, Guang M. Truss optimization on shape and sizing with frequency constraints based on genetic algorithm, *Comput Mech* 2005; **35**(5): 361-8. https://doi.org/10.1007/s00466-004-0623-8
45. Gomes HM. Truss optimization with dynamic constraints using a particle swarm algorithm, *Expert Syst Appl* 2011; **38**(1): 957-68. https://doi.org/10.1016/j.eswa.2010.07.086
46. Miguel LF, Miguel LF. Shape and size optimization of truss structures considering dynamic constraints through modern metaheuristic algorithms, *Expert Syst Appl* 2012; **39**(10): 9458-67. https://doi.org/10.1016/j.eswa.2012.02.113
47. Kaveh A, Hamedani KB, Kamalinejad M. An enhanced Forensic-Based Investigation algorithm and its application to optimal design of frequency-constrained dome structures, *Comput Struct* 2021; **256**: 106643. https://doi.org/10.1016/j.compstruc.2021.106643
48. Kaveh A, Hamedani KB, Kamalinejad M. Improved slime mould algorithm with elitist strategy and its application to structural optimization with natural frequency constraints, *Comput Struct* 2022; **264**: 106760. https://doi.org/10.1016/j.compstruc.2022.106760
49. Kaveh A, Ilchi Ghazaan M. Vibrating particles system algorithm for truss optimization with multiple natural frequency constraints, *Acta Mech* 2017; **228**(1): 307-22. https://doi.org/10.1007/s00707-016-1725-z
50. Kaveh A, Zolghadr A. Meta-heuristic methods for optimization of truss structures with vibration frequency constraints, *Acta Mech* 2018; **229**(10): 3971-92. https://doi.org/10.1007/s00707-018-2234-z
51. Kaveh A, Zolghadr A. Cyclical parthenogenesis algorithm for layout optimization of truss structures with frequency constraints, *Eng Optim* 2017; **49**(8): 1317-34. https://doi.org/10.1080/0305215X.2016.1245730
52. Kaveh A, Biabani Hamedani K, Barzinpour F. Optimal size and geometry design of truss structures utilizing seven meta-heuristic algorithms: a comparative study, *Int J Optim Civ Eng* 2020; **10**(2), 231-60.
53. Griffiths, D. J. (2005). Introduction to quantum mechanics. *2nd, Pearson, Chapter2. The time-independent schrodinger equation*, 90-91.
54. Khatibinia M, Naseralavi SS. Truss optimization on shape and sizing with frequency constraints based on orthogonal multi-gravitational search algorithm, *J Sound Vib* 2014; **333**(24): 6349-69. https://doi.org/10.1016/j.jsv.2014.07.027
55. Talbi EG. *Metaheuristics: from design to implementation*, 1st edition, John Wiley & Sons, 2009.
56. Kaveh A. *Advances in metaheuristic algorithms for optimal design of structures*, 3rd edition, Springer International Publishing, 2021.
57. Joines JA, Houck CR. On the Use of Non-Stationary Penalty Functions to Solve Nonlinear Constrained Optimization Problems with GA's. InInternational Conference on Evolutionary Computation 1994 (pp. 579-584). https://doi.org/10.1109/ICEC.1994.349995
58. Kulkarni O, Kulkarni N, Kulkarni AJ, Kakandikar G. Constrained cohort intelligence using static and dynamic penalty function approach for mechanical components design, *Int J Parallel Emergent Distrib Syst* 2018; **33**(6): 570-88. https://doi.org/10.1080/17445760.2016.1242728
59. Jordehi AR. A review on constraint handling strategies in particle swarm optimisation, *Neural Comput Appl* 2015; **26**(6): 1265-75. https://doi.org/10.1007/s00521-014-1808-5

60. Kaveh A, Ilchi Ghazaan M. *Meta-heuristic algorithms for optimal design of real-size structures*, 1st edition, Springer International Publishing, 2018.
61. Kaveh A, Ilchi Ghazaan M. Optimal design of dome truss structures with dynamic frequency constraints, *Struct Multidiscip Optim* 2016; **53**(3): 605-21. https://doi.org/10.1007/s00158-015-1357-2
62. Kaveh A, Ilchi Ghazaan M. A new hybrid meta-heuristic algorithm for optimal design of large-scale dome structures, *Eng Optim* 2018; 50(2): 235-52. https://doi.org/10.1080/0305215X.2017.1313250
63. Degertekin SO, Bayar GY, Lamberti L. Parameter free Jaya algorithm for truss sizing-layout optimization under natural frequency constraints, *Comput Struct* 2021; **245**: 106461. https://doi.org/10.1016/j.compstruc.2020.106461
64. Kaveh A, Hamedani KB, Joudaki A, Kamalinejad M. Optimal analysis for optimal design of cyclic symmetric structures subject to frequency constraints, *Structures* 2021; **33**: 3122-36. https://doi.org/10.1016/j.istruc.2021.06.054